Journal of Civil and Hydraulic Engineering
https://www.acadlore.com/journals/JCHE

Assessment of Ultra-High Performance Concrete Mechanical Properties and Damage Under Low-Temperature Curing Conditions

Lei Zhang[1*], Yanwei Shi[1,2], Guanying Liu[3]

[1] Yellow River Institute of Hydraulic Research, YRCC, Henan Engineering Research Center of Hydropower Engineering Abrasion Test and Protection, 450003 Zhengzhou, China
[2] College of Water Conservancy and Hydropower Engineering, Hohai University, 210098 Nanjing, China
[3] Sanmenxia Yellow River Mingzhu Group Ltd, 472000 Sanmenxia, China

* Correspondence: Lei Zhang (hkyzhanglei@163.com)

Received: 09-05-2023 **Revised:** 10-20-2023 **Accepted:** 10-26-2023

Citation: L. Zhang, Y. W. Shi, and G. Y. Liu, "Assessment of Ultra-High Performance Concrete mechanical properties and damage under low-temperature curing conditions," *J. Civ. Hydraul. Eng.*, vol. 1, no. 1, pp. 1–10, 2023. https://doi.org/10.56578/jche010101.

Abstract: In regions characterized by extreme cold and elevated altitudes, notably in the northwest, the mechanical characteristics of construction materials such as Ultra-High Performance Concrete (UHPC) are critically impacted by ambient temperatures. This study investigates the mechanical properties of UHPC subjected to low-temperature curing environments, conducting uni-axial compressive and splitting tensile strength tests on UHPC specimens, which comprise water, dry mix, and steel fibers. These specimens were cured at varied temperatures (-10℃, -5℃, 5℃, 10℃). Utilizing damage theory principles, the loss rate in compressive strength of UHPC post-curing was quantified as a damage indicator, revealing internal degradation. A predictive model for damage under low-temperature maintenance was developed, grounded in the two-parameter Weibull probability distribution and empirical damage models. Parameter estimation for this model was achieved through the least squares method, informed by experimental data. The findings indicate a rapid increase in UHPC's mechanical strength at all curing temperatures, with 7-day strength achieving approximately 90% of its 28-day counterpart. A positive correlation was observed between the mechanical strength of UHPC, curing temperature, and age. Despite a reduction in mechanical strength due to low-temperature curing, UHPC was found to attain anticipated strength levels suitable for construction in cold environments. The proposed model for predicting UHPC damage under low-temperature conditions demonstrated efficacy in estimating the strength loss rate, thereby offering substantial technical support for UHPC's application in northwest regions.

Keywords: Ultra-High Performance Concrete (UHPC); Low-temperature curing; Mechanical properties; Compressive strength loss rate; Damage prediction model; Least squares method

1 Introduction

UHPC, a novel cement-based composite material, exhibits distinct properties compared to traditional concrete [1]. The strength enhancement mechanism in UHPC is attributed to the increased compactness of the concrete matrix and the augmented bridging effect of fibers, which effectively impedes crack progression [2, 3]. With the ongoing implementation of China's western development strategy, numerous construction projects are being executed in regions characterized by low temperatures, high cold, and elevated altitudes. In these environments, concrete often develops significant cracking, adversely affecting its durability and crack resistance. Such degradation in early-stage concrete can compromise structural integrity and pose safety risks, ultimately reducing the lifespan of infrastructure [4].

Traditionally, concrete components are cured at room temperature, a process applicable across various environmental conditions. However, in the practical context of the northwest region, a majority of concrete structures necessitate curing under low-temperature conditions. The mechanical properties of concrete materials under such conditions have been relatively under-researched, prompting scholars to investigate the influence of curing temperature on these properties. Mechanical performance tests conducted under variable, high, and low-temperature curing conditions have revealed substantial degradation in the mechanical properties of concrete when cured in a

low-temperature environment [5–7]. It has been observed that low temperatures impede the hydration reaction in concrete, diminishing its strength and increasing susceptibility to deformation and damage [8]. In pursuit of deeper insights into the effects of low-temperature curing, studies by Lu et al. [9] and Kim et al. [10, 11] have examined concrete's mechanical performance at different curing ages under such conditions. These studies confirm that both the curing temperature and the duration of curing positively influence the compressive strength and elastic modulus of concrete, thereby underscoring the potential detrimental effects of low-temperature curing on concrete's structural properties.

While numerous studies have focused on the behavior of ordinary concrete under varying curing temperatures, research on new materials such as UHPC remains relatively limited. This gap is particularly notable in the context of promoting UHPC application in the northwest region, characterized by its challenging low-temperature environment. To address this, the present study embarks on an experimental and theoretical exploration of the alterations in UHPC's mechanical properties under low-temperature curing conditions. Investigations were conducted through uni-axial compressive tests and splitting tensile tests on UHPC samples cured at temperatures of -10°C, -5°C, 5°C, and 10°C. Central to this research is the development of a low-temperature maintenance damage prediction model. This model utilizes the rate of compressive strength loss as a key variable, aiming to provide critical technical support for the construction and maintenance of UHPC structures in low-temperature environments.

2 Methods and Materials

In the investigation of UHPC mechanical properties under low-temperature curing conditions, a total of 45 samples for both compressive and splitting tensile tests were prepared. Each set comprised three test blocks, standardized to a geometric size of 100mm ×100mm×100mm. Uniformity in the test results was ensured by fabricating all test blocks from the same batch, maintaining a consistent material ratio. The UHPC mixture, supplied by Beijing SINO-SINR, adhered to the specific ratio detailed in Table 1, with steel fiber parameters as outlined in Table 2. The methodology for testing incorporated an electronic universal testing machine. Compressive tests were executed at a loading speed ranging from 18-30MPa/min, while splitting tensile tests were conducted at speeds of 1.8-3.6MPa/min.

Table 1. UHPC mix ratio ($1m^3$)

Volume Content of Steel Fibers / %	Dry Mix /kg	Water /kg	Steel Fibers /kg
2%	2045	253	156

Table 2. Main properties of steel fibers

Length /mm	Diameter /mm	Tensile Strength/MPa	Elastic Modulus /GPa
13	0.23	$\geq$ 2000	200

Table 3. Test plan and group number

Table A-Compressive Test					
Group Number	Curing Temperature /°C	Group-Number	Curing Temperature /°C	Group-Number	Curing Temperature /°C
A01-3	20	A01-7	20	A01-28	20
A02-3	10	A02-7	10	A02-28	10
A03-3	5	A03-7	5	A03-28	5
A04-3	-5	A04-7	-5	A04-28	-5
A05-3	-10	A05-7	-10	A05-28	-10
Table B-Splitting Tensile Test					
Group Number	Curing Temperature /°C	Group Number	Curing Temperature /°C	Group-Number	Curing Temperature /°C
B01-3	20	B01-7	20	B01-28	20
B02-3	10	B02-7	10	B02-28	10
B03-3	5	B03-7	5	B03-28	5
B04-3	-5	B04-7	-5	B04-28	-5
B05-3	-10	B05-7	-10	B05-28	-10

UHPC test blocks were fabricated in accordance with the guidelines outlined in the Reactive Powder Concrete (GB/T 31387-2015) [12] and the Hydraulic Concrete Test Code (SL 352-2006) [13], with necessary modifications. The dry mixture was initially stirred for 1 minute, followed by the addition of water and further stirring for 5-7 minutes until reaching a liquid state. Steel fibers were then gradually introduced, with continuous stirring for an additional 8-10 minutes prior to pouring into molds. After a 12-hour room temperature storage period, the test blocks were relocated to various temperature environments for curing. The categorization of test samples was conducted as depicted in Table 3, dividing them into two main groups based on the mechanical performance testing plan: Group A for compressive tests and Group B for splitting tensile tests. Group A was further divided into five subgroups (A01, A02, A03, A04, A05) based on curing temperature, with subgroup numbers representing specific curing temperatures. Post-curing, specimens underwent compressive tests, segmented into A-3, A-7, and A-28 groups according to the curing age, where the numbers represent the respective days of curing. For instance, A01-3 denotes UHPC specimens tested for compressive strength after a 3-day curing at 20°C. Group B, designated for splitting tensile tests, followed a similar grouping methodology as Group A.

3 Results

3.1 Compressive Strength Test

Uniaxial compressive strength tests were systematically performed on UHPC specimens under varied curing temperatures. Figures 1 and 2 illustrate the typical failure morphology of these UHPC specimens at different ages.

(a) 3d (b) 7d (c) 28d

Figure 1. Failure morphology of UHPC compressive tests at different ages under 20℃ curing

(a) 3d (b) 7d (c) 28d

Figure 2. Failure morphology of UHPC compressive tests at different ages under -10℃ curing

Observations, as depicted in Figures 1 and 2, reveal that upon damage, UHPC specimens predominantly exhibit penetrating cracks. A notable increase in the number and width of these cracks is evident with decreasing curing temperatures. Moreover, in specimens with a shorter curing age, superficial peeling of fragments is observed. However, it is crucial to note that, in contrast to conventional concrete, the presence of steel fibers in UHPC mitigates the extent of fragment peeling, thereby preserving overall structural integrity.

Table 4. Standard compressive strength of UHPC at different curing temperatures and ages

Number	Strength/MPa	Number	Strength/MPa	Number	Strength/MPa
A01-3	82.08	A01-7	105.85	A01-28	120.16
A02-3	75.15	A02-7	94.07	A02-28	102.11
A03-3	70.94	A03-7	87.74	A03-28	90.22
A04-3	63.54	A04-7	75.81	A04-28	80.01
A05-3	60.32	A05-7	66.24	A05-28	73.00

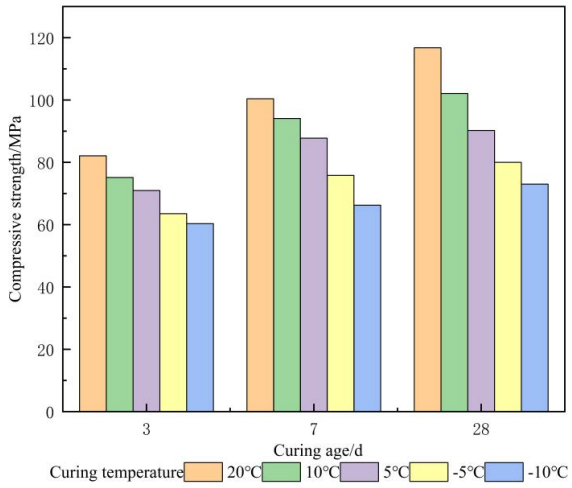

Figure 3. Relationship between UHPC compressive strength and curing age under different curing temperatures

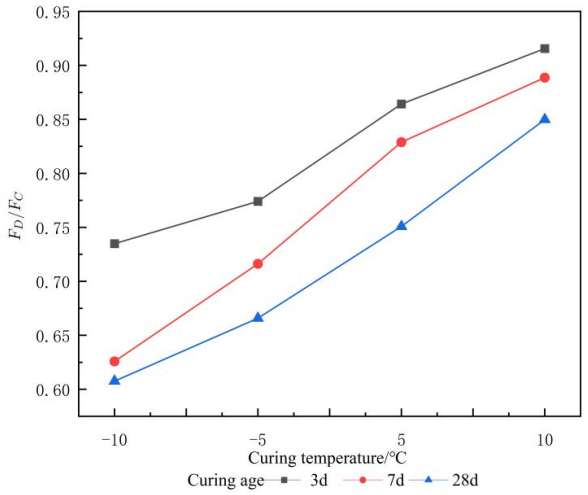

Figure 4. Relationship between F_D/F_C ratio and curing temperature

Comprehensive data from the compressive strength tests of UHPC at various curing temperatures and ages are systematically presented in Table 4. These data underpin the construction of a histogram (Figure 3), elucidating the relationship between UHPC compressive strength and curing age across different temperatures. Additionally, Figure 4 provides a line graph delineating the relationship between the compressive strength of UHPC under varied low-temperature curing conditions (F_D), room temperature curing conditions (F_C), and the corresponding curing temperatures (T).

Figures 3 and 4 graphically represent the experimental results. Notably, the early strength of UHPC is observed to escalate swiftly, with the strength at 7 days achieving approximately 90% of that at 28 days. This rapid increase in early strength is attributed to the composition of UHPC, predominantly comprising fine-grained aggregates. The integration of steel fibers plays a pivotal role in enhancing inter-aggregate connectivity. This results in a reduction in internal porosity, an increase in density, and an augmented hydration reaction, collectively contributing to the rapid strength gain. With the progression of time, a distinct variation in compressive strength of UHPC is observed under different curing temperatures. A consistent trend emerges: as curing temperatures decline, compressive strength correspondingly decreases. The most substantial decline is witnessed under a curing regime of -10℃, where the 28-day strength is reduced to merely 60.75% of the strength observed under room temperature curing. This phenomenon parallels the hydration behavior observed in ordinary concrete [8]. Lower temperatures are found to mitigate the hydration effect, a factor exacerbated at sub-zero temperatures where the freezing and expansion of water within

UHPC induces internal structural damage, thus significantly diminishing compressive strength. Contrastingly, UHPC demonstrates a remarkable capacity to retain high compressive strength even following low-temperature curing. An exemplary instance is the achievement of 60MPa in strength following a 3-day curing period at -10℃, substantially surpassing the strength typically expected from ordinary concrete components. This attribute of UHPC negates the necessity for hot curing processes in cold construction environments, offering significant reductions in both construction and long-term operational and maintenance costs for enterprises.

3.2 Splitting Tensile Strength Test

The splitting tensile strength of UHPC was evaluated under varying curing conditions. Figures 5 and 6 depict the characteristic failure patterns of UHPC specimens during these tests. It was observed that failure typically occurs at the midpoint of the specimen, with vertical cracks developing along the load direction. Notably, upon reaching peak load capacity, one of these cracks predominantly widens. However, unlike ordinary concrete, the presence of steel fibers within UHPC maintains a degree of connectivity between the cracked segments, thereby exhibiting ductility.

(a) 3d (b) 7d (c) 28d

Figure 5. Morphology of UHPC failure under splitting tensile test at various ages with 20°C curing

(a) 3d (b) 7d (c) 28d

Figure 6. Morphology of UHPC failure under splitting tensile test across different ages with -10°C curing

A series of splitting tensile tests were conducted on UHPC blocks subjected to different curing temperatures and ages. For each set of conditions, three replicates were tested to ensure reliability, and the average result was recorded, as detailed in Table 5. Subsequent to the tests, the relationship between the splitting tensile strength and curing age for different temperatures was plotted, as illustrated in Figure 7. The findings can be summarized as follows:

(1) Influence of low-temperature curing on strength increment rate: The experimental data indicate a notable decline in the rate of increase in splitting tensile strength of UHPC specimens subjected to low-temperature curing. Specifically, at a curing temperature of 20℃, the average splitting tensile strength values at 3, 7, and 28 days were 7.79 MPa, 9.73 MPa, and 10.52 MPa, respectively. This corresponds to a 35.0% increase in strength over the 28-day period. In contrast, the strength increment for specimens cured at temperatures of -10℃, -5℃, 5℃, and 10℃ over the same period were 17.6%, 22.5%, 25.5%, and 28.0%, respectively. Thus, it is evident that low-temperature curing slows the rate of increase in splitting tensile strength, with the most significant impact observed under negative temperature conditions

(2) Impact on Splitting Tensile Strength: The data further reveal that low-temperature curing substantially reduces the splitting tensile strength of UHPC specimens. For instance, at 28 days, specimens cured at 20℃ displayed increases in splitting tensile strength of 54.3%, 42.2%, 23.6%, and 12.2% when compared to specimens cured at -10℃, -5℃, 5℃, and 10℃, respectively. This trend underscores the detrimental effect of lower temperatures on splitting tensile strength, which is possibly attributable to the diminished hydration reaction at lower temperatures, leading to weaker adhesion between steel fibers and the cementitious matrix, thereby reducing the fibers' effectiveness in crack suppression.

Table 5. Splitting tensile strength of UHPC at different curing temperatures and ages

Curing Temperature / °C	Number	Strength/MPa	Number	Strength/MPa	Number	Strength/MPa
20	B01-3	7.79	B01-3	9.73	B01-28	10.52
10	B02-3	7.33	B02-3	8.62	B02-28	9.38
5	B03-3	6.78	B03-3	7.71	B03-28	8.51
-5	B04-3	6.04	B04-3	6.61	B04-28	7.40
-10	B05-3	5.80	B05-3	6.23	B05-28	6.82

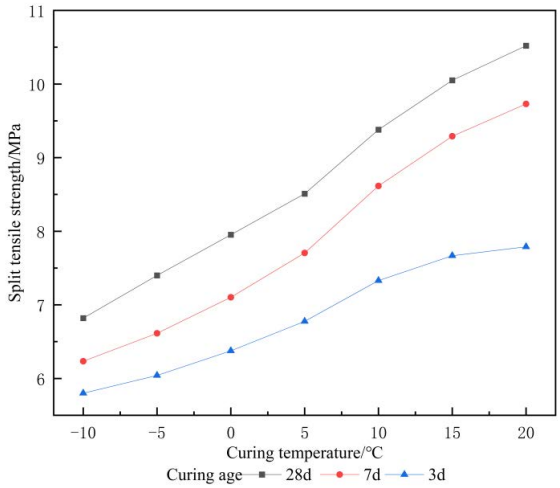

Figure 7. Relationship between splitting tensile strength and curing temperature of UHPC at different curing ages

4 UHPC Damage Prediction Model under Low Temperature Curing

UHPC is a heterogeneous cementitious composite material, and the development of damage prediction models under various operational conditions is pivotal for understanding its failure mechanisms and predicting its structural integrity. This section establishes a damage prediction model for UHPC post low-temperature curing, derived from the previously mentioned relationship between the curing temperature and the compressive strength. The model's accuracy is substantiated by experimental data.

4.1 Damage Prediction Model

The degradation of compressive strength is a principal metric for assessing damage in such materials. The proposed damage model for UHPC, post low-temperature curing, is represented by Eq. (1):

$$D^{(t)} = 1 - F_D/F_C \tag{1}$$

where, $D^{(t)}$ denotes the damage value of UHPC after different low-temperature curing, F_D represents the compressive strength after low-temperature curing, F_C is the compressive strength after room temperature curing.

Given the inherent material heterogeneity of UHPC, its cumulative damage under low-temperature conditions exhibits stochastic characteristics. Consequently, a probabilistic approach is more suitable for this analysis. The Weibull distribution, commonly employed in prediction analysis and reliability engineering, is particularly apt for modeling the variability observed in UHPC damage under low-temperature conditions. The two-parameter Weibull distribution function applied in this context is delineated in Eq. (2):

$$D_{(t)} = 1 - \exp\left[-(\lambda t)^{\beta}\right] \tag{2}$$

4.2 Model Parameter Estimation

The parameter estimation for the damage prediction model of UHPC under low-temperature curing presents unique challenges. The extended duration required for low-temperature curing results in a limited dataset, necessitating an approach that is both precise and adaptable to smaller samples. In this context, the least squares method, renowned

for its high accuracy and practicality, is employed to estimate the unknown parameters within the framework of small sample data and the Weibull distribution function [14].

Initially, data normalization is conducted. To mitigate the influence of negative values, it is imperative to standardize the data within a $[1, 2]$ interval range:

$$k = (2-1)/\left(t_{\text{Max}} - t_{\text{Min}}\right) \tag{3}$$

$$t_{new} = 1 + k\left(t - t_{\text{Min}}\right) \tag{4}$$

Subsequent transformations are applied to Eq. (2):

$$1 - D_{(t)} = \exp\left[-\left(\lambda t_{new}\right)^{\beta}\right] \tag{5}$$

$$\frac{1}{1 - D_{(t)}} = \exp\left[\left(\lambda t_{new}\right)^{\beta}\right] \tag{6}$$

$$\ln\left[\ln\frac{1}{1 - D_{(t)}}\right] = \beta\ln(\lambda) + \beta\ln\left(t_{\text{new}}\right) \tag{7}$$

Assuming $y = \ln\left[\ln\frac{1}{1-D_{(t)}}\right]$, $\quad x = \ln\left(t_{\text{new}}\right)$, $\quad a = \beta$, $\quad b = \beta\ln(\lambda)$, a linear function can be derived:

$$y = ax + b \tag{8}$$

4.3 Verification of Damage Prediction Model

The applicability and accuracy of the damage prediction model for UHPC under low-temperature curing conditions were rigorously evaluated. The necessary parameters for this evaluation were derived through linear fitting, utilizing the Origin software, as depicted in Figure 8. The resulting slope and intercept of the linear fit correspond to the estimated values of parameters β and λ in the Weibull distribution model. The coefficient of determination $\left(\mathrm{R}^2\right)$ serves as an indicator of the fit quality of the model parameters, and these specific parameters are detailed in Table 6.

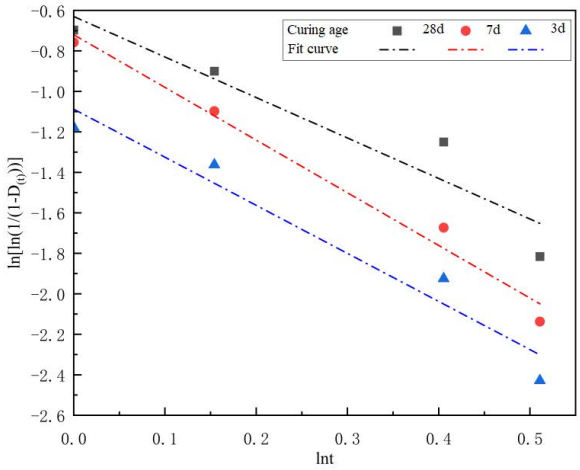

Figure 8. Least squares parameter fitting of UHPC compressive strength degradation data

By incorporating these parameters into the established UHPC damage prediction model, the evolution functions for UHPC damage under various curing ages and low-temperature conditions were calculated, as shown in Table 7. The model's validity was then assessed by comparing the calculated values from the model against the actual experimental values, with these comparisons illustrated in Figure 9.

Table 6. Weibull parameter distribution values

Curing age	a	b	β	λ	$\mathbf{R^2}$
3 d	-2.3750	-1.0878	-2.3750	1.5809	0.9496
7 d	-2.3530	-0.8001	-2.3530	1.4050	0.9821
28 d	-2.3003	-0.6301	-2.3003	1.3151	0.9037

Table 7. Damage evolution function of UHPC

Curing age	Damage Evolution Function
3d	$D_{(t)} = 1 - \exp\left[-(1.5809t_{new})^{-2.3750}\right]$
7d	$D_{(t)} = 1 - \exp\left[-(1.4050t_{new})^{-2.3530}\right]$
28d	$D_{(t)} = 1 - \exp\left[-(1.3151t_{new})^{-2.3003}\right]$

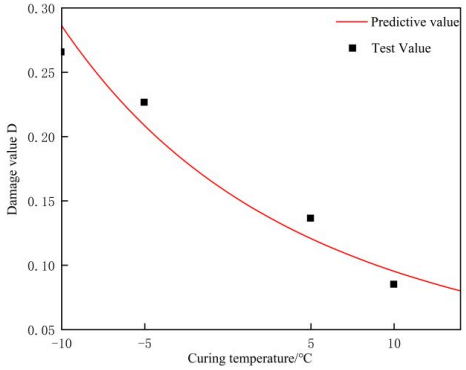

(a) 3d

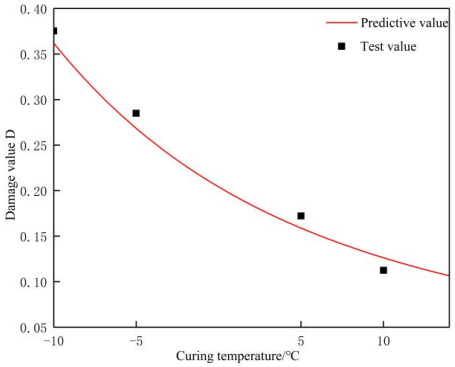

(b) 7d

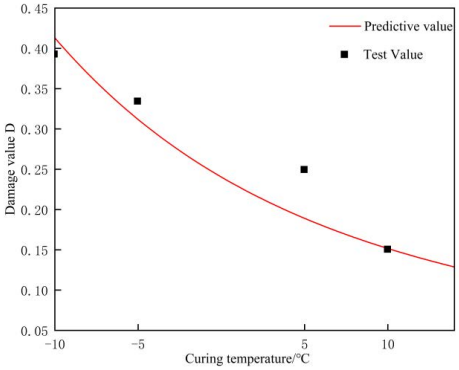

(c) 28d

Figure 9. Comparison diagram of damage value D-curing temperature relationship under different curing ages

The analysis of Figure 9 reveals a strong correlation between the calculated damage evolution function curves and the experimental data, demonstrating the model's robust predictive capability. This congruence underscores the model's efficacy in accurately reflecting the interplay between UHPC curing temperature and damage values across different curing ages. Consequently, this model serves as a reliable tool for predicting the longevity of UHPC under low-temperature curing conditions. The results further suggest that curing temperature significantly influences the mechanical property recovery of UHPC, with an observed gradual increase in strength under low-temperature conditions. Thus, the developed model offers valuable insights into determining optimal construction times by

predicting UHPC damage under low-temperature conditions and aligning these predictions with local temperature variations.

5 Conclusions

In the investigation of the influence exerted by low-temperature curing conditions on the mechanical properties of UHPC, extensive tests were conducted to assess both uni-axial compressive strength and splitting tensile strength. The salient findings from these tests are summarized as follows:

(1) A rapid increase in the strength of UHPC was observed, with the strength at 7 days reaching approximately 90% of that at 28 days. A positive correlation between strength, curing temperature, and curing age was noted. The impact of negative temperature curing was found to be considerably pronounced on the mechanical strength of UHPC. At -10℃, the mechanical strength of UHPC was approximately half of that observed at room temperature, while the reduction in mechanical strength at temperatures above 0℃ was less than 20%. Thus, it is advised to conduct construction activities at temperatures above 0℃ to significantly enhance the mechanical properties of concrete.

(2) Notably, UHPC demonstrated substantial compressive strength even after low-temperature curing. The strength achieved after 3 days of curing at -10℃ was recorded at 60 MPa, surpassing the expected strength of conventional concrete components. This finding suggests that UHPC can forego the thermal maintenance process typically required in low-temperature construction environments, potentially leading to considerable savings in both construction costs and later operational and maintenance expenses.

(3) The UHPC damage prediction model developed in this study exhibited a robust correlation with empirical values. This model can reliably predict the damage values of concrete under low-temperature construction conditions, offering vital technical support for the broader application of UHPC, particularly in Northwest China. However, this study did not encompass the mechanical property testing of UHPC under dynamic curing temperatures, a topic that merits exploration in subsequent research. Future investigations should aim to provide precise and viable methodologies for understanding the variation in mechanical properties of UHPC with fluctuating curing temperatures.

Funding

This paper was funded by Funder National Natural Science Foundation of China (Grant No.: 52279134), Fundamental research funds for the central nonprofit research institutions (Grant No.: HKY-JBYW-2022-01), and Jiangsu Postgraduate Research & Practice Innovation Program of Jiangsu Province (Grant No.: SJCX22_0183).

Data Availability

The data used to support the findings of this study are available from the corresponding author upon request.

Conflicts of Interest

The authors declare that they have no conflicts of interest.

References

[1] B. C. Chen, T. Ji, Q. W. Huang, H. Z. Wu, Q. J. Ding, and Y. W. Zhan, "Review of research on ultra-high performance concrete," *J. Archit. Civ. Eng*, vol. 31, pp. 1–24, 2014.

[2] M. T. Hasan, S. Allena, Y. Sharma, and M. Yeluri, "Effect of fine aggregate particle size on physical, mechanical, and durability properties of ultra-high performance concrete," *Transp. Res. Rec.*, vol. 2676, no. 5, pp. 820–830, 2022. https://doi.org/10.1177/03611981211072854

[3] J. Wang, S. Dong, D. S. Pang, X. Yu, B. Han, and J. Ou, "Tailoring anti-impact properties of ultra-high performance concrete by incorporating functionalized carbon nanotubes," *Eng.*, vol. 18, no. 11, pp. 232–245, 2021. https://doi.org/10.1016/j.eng.2021.04.030

[4] M. Husem and S. Gozutok, "The effects of low temperature curing on the compressive strength of ordinary and high performance concrete," *Constr. Build. Mater.*, vol. 19, no. 1, pp. 49–53, 2005. https://doi.org/10.1016/j.conbuildmat.2004.04.033

[5] L. Zhang, Z. Wang, J. Tong, H. Zhang, G. Wu, and Z. Cao, "Influence of curing environment on restricted shrinkage cracking of concrete," *J. Water Resour. Water Eng.*, vol. 33, no. 3, pp. 156–162, 2022. https://doi.org/10.11705/j.issn.1672-643X.2022.03.20

[6] J. Zhang, S. Peng, W. Li, S. Wang, Q. Wang, X. Ling, and Z. Cheng, "Literature review of low temperature performance of concrete," *Build. Struct.*, pp. 1–10, 2023. https://doi.org/10.19701/j.jzjg.20221426

[7] G. Li, B. Li, A. Huang, and J. S. Deng, "Effects of curing temperature and mineral admixtures on brittleness of steam cured concrete," *Bull. Chin. Ceram. Soc.*, vol. 42, no. 2, pp. 487–495, 2023.

[8] P. Ding, Y. Xu, and W. Lin, "Study on the influence of curing temperature on concrete hydration process," *Build. Struct.*, vol. 52, no. S2, pp. 1108–1113, 2022.

[9] J. Lu, J. Liu, H. Yang, J. Gao, X. Wan, and J. Zhang, "Influence of curing temperatures on the performances of fiber-reinforced concrete," *Constr. Build. Mater.*, vol. 339, p. 127640, 2022. https://doi.org/10.1016/j.conbuildmat.2022.127640

[10] J. K. Kim, S. H. Han, and Y. C. Song, "Effect of temperature and aging on the mechanical properties of concrete: Part I. Experimental results," *Cem. Concr. Res.*, vol. 32, no. 7, pp. 1087–1094, 2002. https://doi.org/10.1016/S0008-8846(02)00744-5

[11] J. K. Kim, S. H. Han, and S. K. Park, "Effect of temperature and aging on the mechanical properties of concrete: Part II. Prediction model," *Cem. Concr. Res.*, vol. 32, no. 7, pp. 1095–1100, 2002. https://doi.org/10.1016/S0008-8846(02)00745-7

[12] *Reactive powder concrete*, Std. GB/T 31 387-2015, 2015.

[13] *Test code for hydraulic concrete*, Std. SL 352-2020, 2020.

[14] K. Li, Z. Wei, H. X. Qiao, C. G. Lu, J. Guo, and S. Huang, "Weibull durability life prediction method of reinforced concrete in environment of coupled salt solution," *Acta Mater. Compos. Sin.*, vol. 38, no. 7, pp. 2370–2382, 2021. https://doi.org/10.13801/j.cnki.fhclxb.20201021.001